CAPABILITIES OF THE IRKUTSK INCOHERENT SCATTERING RADAR FOR SPACE DEBRIS STUDIES

Khakhinov V.V., Lebedev V.P., Medvedev A.V., Ratovsky K.G.

Institute of Solar-Terrestrial Physics SD RAS, Russia, 664033, Irkutsk p/o box 291; Lermontov st., 126a, Email: khakhin@iszf.irk.ru

ABSTRACT

The incoherent scattering radar is promising facilities for obtaining low cost routine space debris observations in low Earth orbit [1].
The Irkutsk Incoherent Scatter Radar (IISR) is intended for studying the ionosphere [2]. Simultaneously with ionospheric measurements IISR detects space object (SO) passing through the IISR sector. In each sample series we measure the following of the SO characteristics: range, beam velocity, azimuth angle, elevation, and signal amplitude. Two from six Keplerian elements of the orbit can be defined with high accuracy, they are the inclination and the right ascension of the ascending node of the observed SO. The SO flux is several tens of thousands per month for standard ionospheric measurements.

1. INTRODUCTION

Now standard month ionospheric measurements are coordinated with the international geophysical calendar. The Irkutsk Incoherent Scatter Radar (IIRS) operates up to 4000 h per year for ionospheric measurements.
During standard month ionospheric measurements the space objects (SO) radar signal data sets are selected by a special program module. These data sets are analyzed and recorded as separate files. In each sample series we measure the following characteristics: range, beam velocity, azimuth angle, SO elevation, and signal amplitude. The measurement results are imported into the database. The SO flux is several tens of thousands per one month of standard ionospheric measurements. The routine space debris observations are also useful for the validation of the large-object catalogues.
In the paper we briefly consider signal processing techniques and results of observations COSMOS 2251 before and after collision with IRIDIUM 33 is presented. The comparison of the obtained data with the prediction of catalogued SO crossing the IISR sector IISR is presented.

2. IRKUTSK INCOHERENT SCATTER RADAR

IIRS located in Eastern Siberia (52.88N, 103.26E) is intended for studying the ionosphere. Simultaneously with ionospheric measurements, IISR detects SO passing through the IISR sector. The IISR sector ground projection at range of 6000 km covers the region (64N, 73E), (68N, 103E), (36N, 108E), (36N, 92E).
The IISR is a monostatic pulse radio location station with frequency scanning. Basic parameters of Irkutsk IS radar are presented in Tab. 1.

Table 1. Basic parameters of Irkutsk IS radar

Range of frequencies	154 - 162 MHz
Two transmitters peak power	2.5 - 3.2 MW
Pulse duration	70 - 900 μs
Pulse-repetition rate	24.4 Hz
Antenna power gain	35 dB
Polarization	Linear

The doubly sectionalized receiving-transmitting antenna comprises of the shaping horn (height 20m, aperture angle 32°, aperture size 246x12.2m), separated by the partition into two symmetric sections. Each section has its independent feeder systems and outputs to the receivers.
The spatial distribution of the radiated power (directional pattern) along the major axis of the antenna system is formed independently from each of the sections. The extended waveguide-slot driving system ensures the ~ 0.5° width of the directional pattern (DP) along the major axis with the first sidelobe level of about -17 dB (see Fig. 1).

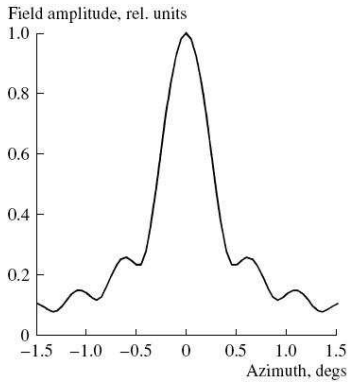

Figure 1. The antenna DP cross section in the azimuth plane

The ribbed retarding structure changes the phase velocity of the wave with a change of the working frequency. This results in a change of the distribution of the initial phases at the radiating slots, i.e. the slope of the phase front. This ensures a scanning of the DP in the plane passing through the major axis of the antenna. At

Proc. '5th European Conference on Space Debris', Darmstadt, Germany 30 March – 2 April 2009, (ESA SP-672, July 2009)

the carrier frequency of 154 MHz it is possible to provide the radiation along the normal to the horn aperture plane. The frequency 154 - 162 MHz frequency range provides the 30° DP deviation from the normal to the horn aperture plane. As the excitation can be fed to a section of the antenna from the both waveguide ends, the total scanning sector is ±30° (See Fig. 2).

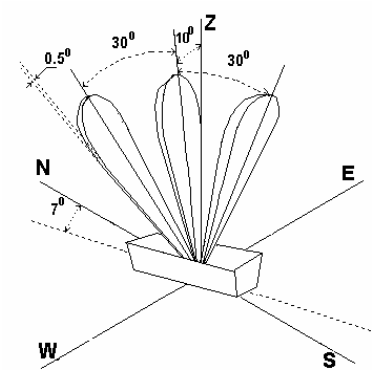

Figure 2. Orientation of IISR antenna system and DP width in-phase composition mode.

Currently only one half of the equipment ensuring the southward direction of the scanning is used.

The width of DP of each of the two sections of the antenna system in the transverse plane (along the short axis of the antenna) is ~ 20° (see Fig. 3). The total radar DP is generated by adding up the DPs of two sections. By varying the phase difference of exciting signals in the antenna sections, it is possible to obtain different total DPs. In the case of in-phase composition, the DP width is ~ 10° in the transverse plane. In this case the antenna gain is twice compared to each of the sections.

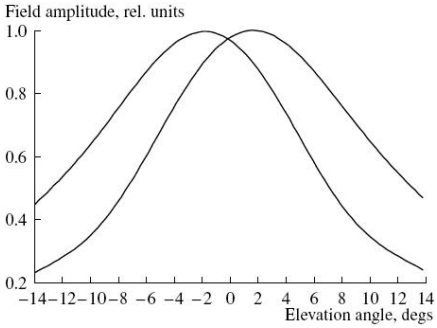

Figure 3. The antenna DP in the plane of the elevation angle in antenna coordinate system

The antenna properties provide enough wide space review for SO detection.

High accuracy for the SO angular coordinate determination can be achieved only with the interference method. The IISR technological modernization provided the possibility of recording signals from the each antenna half-horn and measuring a phase shift between them. The antenna phase-elevation characteristic was measured experimentally by observing such powerful cosmic source as radio galaxy Cygnus-A in the passive mode of cyclic scanning [3]. The resulting phase-elevation characteristic is shown in Fig. 4. The slope of the IISR antenna characteristic is 16 electric degrees per one degree of the elevation angle; this ensures a high accuracy in determining the elevation angle.

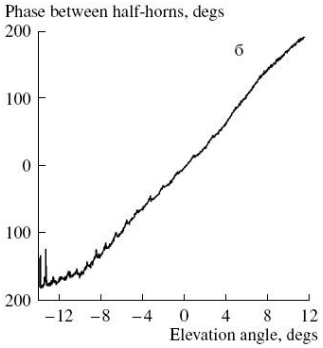

Figure 4. The phase-elevation characteristic of the IISR antenna

The radar energy potential for the detection of SO is characterized by the experimental dependence of the detected object size versus its range at the fixed signal-to-noise-ratio. Fig. 5 presents the radar characteristics obtained by observations of “Starlette”, “Starshine” and “EGP” spherical spacecrafts without coherent accumulation. The total power of the transmitters used in the experiment was 2.2 MW, and the duration of the radiated non-modulated pulse was 750 ms

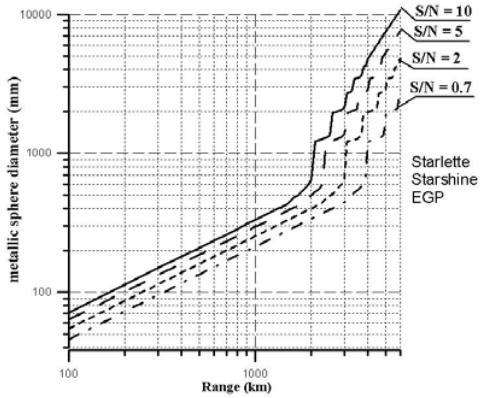

Figure 5. Dependence of the metallic sphere diameter versus its range for different signal-to-noise-ratios.

3. SO DETECTION DURING IISR REGULAR IONOSPHERIC MEASUREMENTS

Since 2005 the regular ionospheric measurements have been carried out in a two-beam mode. Two in-phase transmitters radiate 1.2 MW pulses. For each sounding

step the 750μs rectangular pulse at frequency *f* and the 150μs phase-complex coded pulse at frequency *f+300KHz* are radiated consecutively. Two working frequencies of *f*=154.5 and *f*=159.4 MHz were used. Fig. 6 shows the ground DP projections at -6dB level for the given frequencies and ranges of 300, 800 and 1300 km.

Special observations of selected SO are performed by IISR in automatic "capture – tracking" mode. Phase-complex coded signals of 860μs duration are used. In this mode SO is initially detected by the cyclic beam scanning, then SO is tracked by the beam scanning as long as SO is in the sector.

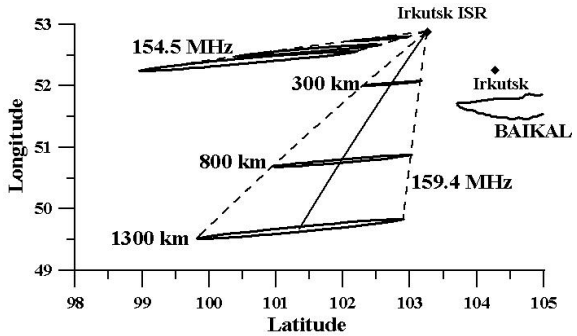

Figure 6. Ground DP projections at -6dB level for the given frequencies and ranges of 300, 800 and 1300 km.

Fig. 7 shows transmitted signals, clutter and IS signal for standard ionospheric measurements.

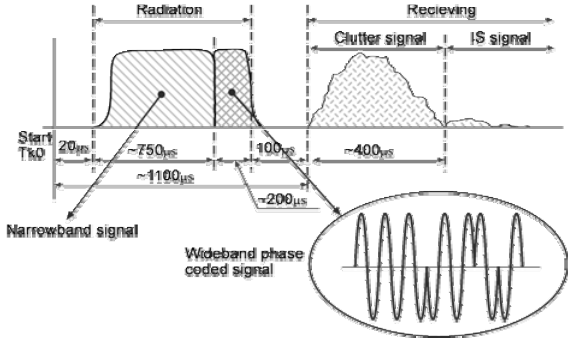

Figure 7. Transmitted signals clutter and IS signal for standard ionospheric measurements.

4. METHOD OF THE SO SELECTION

Let *s(t)* represents complex stationary noise with the normally distributed zero mean quadrature components. The noise power is defined by the average power $\left\langle |s|^2 \right\rangle$ or effective amplitude $\sigma = \sqrt{\left\langle |s|^2 \right\rangle}$.

The noise time-frequency properties are defined by correlation function $R_s(\tau) = \left\langle s(t)s^*(t+\tau) \right\rangle$.

The average frequency f_{th} of crossing of the noise over the threshold level g_{th} is an useful noise characteristic [4]. This characteristic means that a noise crosses the level g_{th} once during time interval $1/f_{th}$ on average, that corresponds to one false alarm during this time interval on average.

Frequency of the threshold crossing can be essentially reduced when the form of the radiated signal is close to rectangular and the flat-top envelope duration T_P is essentially exceed the time interval of noise correlation, i.e. $T_P \Delta F_S >> 1$. The operation of a running average of the reflected signal envelope is defined by expression:

$$\widetilde{g}(t) = \frac{1}{T_p} \int_{t}^{t+T_p} g(\xi) d\xi \,. \qquad (1)$$

The Eq.1 leads to essential change of the noise properties, but the amplitude of the reflected signal does not change.

As a result of integration the noise distribution becomes close to normal and dispersion is reduced proportionally to the duration of the integration interval.

According to [4], the average frequency of crossing of threshold g_{th} for normally distributed noise *s(t)* is defined by expression

$$f_{th}(g_{th}) = \frac{\Omega_S}{2\pi} \exp\left(-\frac{(g_{th} - \langle S \rangle)^2}{2D_S} \right), \qquad (2)$$

where D_S is the dispersion, Ω_S is effective frequency of noise, $\Omega_S^2 = \frac{2}{T_P \tau_s}$.

The Eq.2 allows us to find an explicit expression for level g_{th} for given values of frequency of false alarms f_{th}, time of correlation of noise τ_s, flat-top envelope duration T_P and effective amplitude of noise σ.

$$g_{th} = \sigma \left(\frac{\sqrt{\pi}}{2} + \sqrt{(2 - \frac{\pi}{2}) \frac{\tau_s}{T_p} \ln\left(\frac{1}{\sqrt{2\pi} f_{th} \sqrt{\tau_s T_p}} \right)} \right). \qquad (3)$$

Thus the algorithm of measurement of parameters of the signals reflected from space objects presents the follows steps:

1. Calculation of effective amplitude of noise σ.
2. Calculation of the level g_{th}.
3. Calculation of running average of the envelope $\widetilde{g}(t)$.
4. Definition of the samples series, where $\widetilde{g}(t) > g_{th}$ and recording the samples series in a separate file.

5. Definition of parameters of the signal reflected from SO.

Running the algorithm in real time is the main problem. At present only steps 1-4 are carried out in real time. The definition of parameters of SO movement is performed later from the samples saved in the files. In the next section we consider the method of definition of the SO movement parameters in detail.

5. METHOD OF DEFINITION OF SO MOVEMENT PARAMETERS

The total waveform of the reflected signal is recorded in the form of its two low-frequency quadratures $a(t)$ and $b(t)$. As a result of the digital processing of the radar signals, the parameters of the SO trajectory (range, Doppler velocity, and angles) and some of non-coordinate characteristics are determined.

The technique for determining the reflected signal parameters is based on measuring the complex envelope of the reflected signal $q(t) = a(t) + ib(t)$ and assuming that q(t) has the form:

$$q_j(t) = \mu_j \cdot e^{i(\varphi_j + \omega_j (t-\tau_j))} \begin{pmatrix} q_0(t-\tau_j) + \\ + i\xi_j \dfrac{dq_0(t-\tau_j)}{dt} \end{pmatrix}, \qquad (4)$$

where $q_0(t)$ is the complex envelope of the radiated signal, j - channel number ($j=1$ - west half-horn, $j=2$ - east half-horn), μ, φ, τ, ω and ξ are the amplitude, phase, delay, frequency Doppler shift (FDS) and a parameter associated with additional phase modulation relatively of the radiated signal.

The signal parameters are defined by the minimization of function Δq.

$$\Delta q(\mu, \varphi, \tau, \omega, \xi) = \int_{t_1}^{t_2} \left| q(t) - q_m(t) \right|^2 dt \, . \qquad (5)$$

The delay and FDS are related to the SO coordinate parameters by the follows relations:

$$\tau = 2R/c \, , \;\; \omega = 2\omega_0 V_R / c \, , \qquad (6)$$

where R is the distance from the receive-transmit antenna to SO, c is the light velocity, and V_R is the SO beam velocity.

Relationship of the signal amplitude to the SO parameters is more complicated, it depends on characteristics of the transmitter-receiver channel, SO reflecting properties and SO location in DP.

Phase shift is defined from the maximization of the follows expression:

$$\sum_i (q_1(t_i) + q_2(t_i) e^{i\Delta\varphi})^2 \to \max \, , \qquad (7)$$

where q_1 is the west half-horn signal, q_2 is the east half-horn signal, and $\Delta\varphi$ is the required phase difference. The maximization of the Eq.7 leads to follows expression:

$$\tan \Delta\varphi = \frac{\sum_i a_1(t_i) b_2(t_i) - a_2(t_i) b_1(t_i)}{\sum_i a_1(t_i) a_2(t_i) + b_1(t_i) b_2(t_i)} \, . \qquad (8)$$

The SO elevation angle in the antenna coordinate system is defined by the phase difference $\Delta\varphi$ between signals from the west and east half-horns. In $\pm 12^0$ range of the antenna elevation, it is possible to consider the phase-elevation characteristic is close to linear one (that corresponds to effective interferometer with 4.6m base). Thus the antenna elevation can be defined:

$$\Theta = \Delta\varphi / 16 \, . \qquad (9)$$

The IISR is radar with frequency scanning, i.e. its current azimuth $\varepsilon(f)$ is determined by the working frequency. The SO location at angular distance $\varepsilon(f)$ from the DP center induces the received signal distortions in the in the form of additional phase modulation ($b(t)$ quadrature in Fig. 8) whose amplitude is proportional to $\Delta\varepsilon$ and the shape corresponds to the derivative of the envelope of an emitted signal, i.e. $\xi = \xi(\Delta\varepsilon)$.

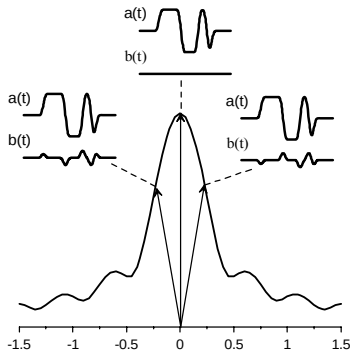

Figure 8. Variation of the signal shape when the target deviates from the DP center in the azimuth plane.

Thus, on the base of technique described above we measured the following SO coordinate characteristics: distance (R), beam velocity (V), azimuth angle (ε),

elevation (Θ), and signal amplitude. When signal-to-noise ratio is high enough (S/N > 10), the typical root mean square deviations for R, V, ε , and Θ are 100 m, 10 m/s, 5 angular minutes, and 5 angular minutes, respectively. This accuracy is enough for determination of the SO orbit in the next SO circuit passing through IISR sector. The SO measurements for two successive circuits provide a more precise determination of the SO orbit.

6. THE IISR OBSERVATIONS OF COSMOS 2251 BEFOR AND AFRTER COLLISION WITH IRIDIUM 33

It is known, that Cosmos 2251 and Iridium 33 satellites are collided at the altitude of 790 km on February 10, 2009 at 16:56 UT. From 21 January to 18 February the IISR regular ionospheric measurements were conducted. Results of collision have been recorded by IISR after several days. Time intervals corresponded to Cosmos 2251 crossing the IISR sector before and after collision have been found by Keplerian elements of the orbit. Results of the observations of Cosmos 2251 at 10:31:46 – 10:31:58 UTC interval on February 09, 2009 and 09:34:21 – 09:35:50 UTC interval on February 14, 2009 are shown in figure 9. The top panels of Fig. 9a and 9d show the signal amplitudes.

The amplitude dynamics of the signal from Cosmos 2251 are given in relative unities, different colors corresponds to dynamics of SO passing through DP at different sounding frequencies (azimuths). The antenna side-lobe structure is clearly visible.

The middle panel shows the measured slant range (small circles) and the catalogue prediction (linear). The bottom panel shows the measured Doppler velocity (small circles) and the catalogue prediction for this parameter (linear). Fig. 9a, 9b, 9c and Fig. 9d, 9e, 9f show the results of the observations obtained before and after the collision, respectively. One can see that there are four new objects with elements of orbits missing in the catalogue. Thin solid lines present the predicted range and velocity values of the catalogued SO.

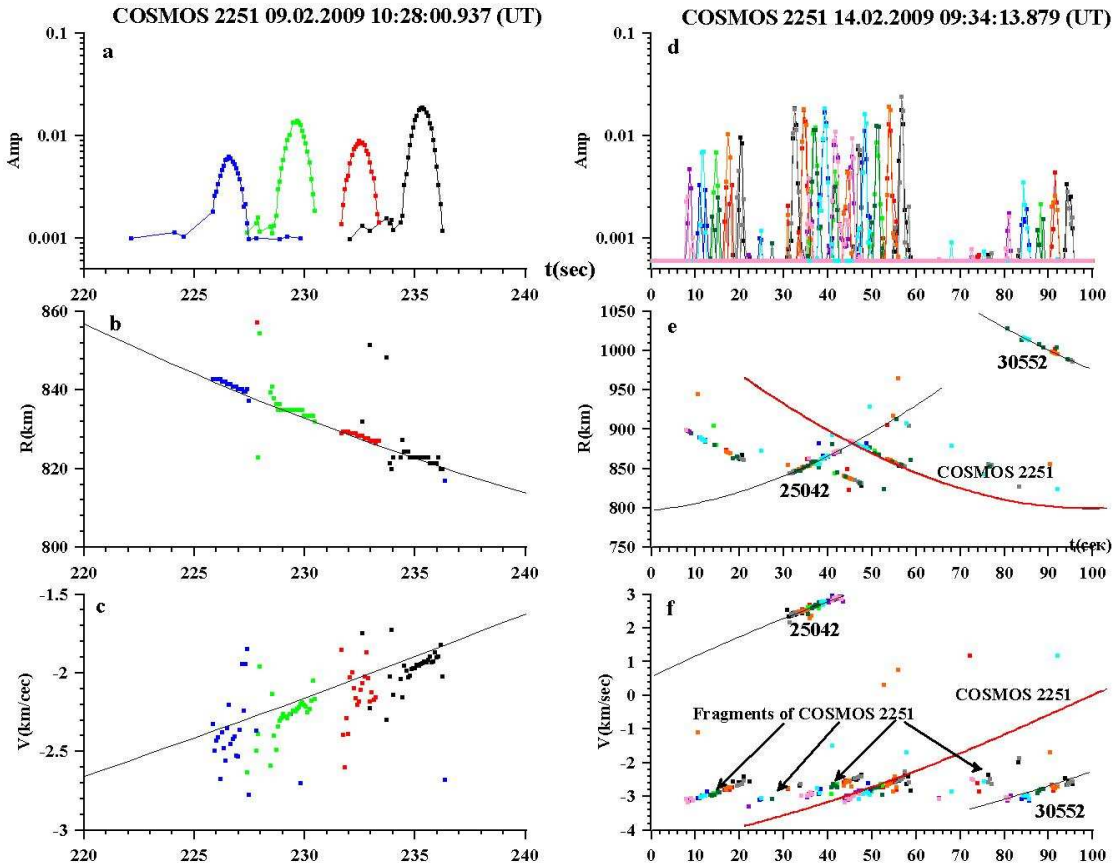

Figure 9. Passes of catalogued object Cosmos 2251 at 10:31:46 – 10:31:58 UTC on 09 February 2009 and 09:34:21 – 09:35:50 UTC on 14 February 2009, compared against the TLE prediction. The top panel shows the signal amplitude. The middle panel shows the measured slant range (small circles) and the catalogue prediction (linear). The bottom panel shows the measured Doppler velocity (small circles) and the catalogue prediction (linear).

7. RESULTS OF THE COMPARISON WITH THE CATALOGUE PREDICTION

We recorded several tens of thousands of space objects (SO) flights during the latest experiment in February 2009, i.e. about 40-60 flights per hour and more than 1100 flights per day. For the comparison with the catalogue prediction we used the SO orbit data in the form of TLE from the Space-Track web site, www.space-track.org. According to the catalogue, more than 9000 SO may pass through the IISR sector. For each of these SO we calculated the ephemerid and path characteristics relatively to IISR. As a result we obtained the altitude distribution of both observed and calculated from the catalogue SO. These distributions are shown in Fig. 10 and 11 for February 14 and 16 of 2009, respectively. The blue histograms show the distributions of the calculated SO satisfying two conditions: (1) the SO ephemerid has to pass through at least one of the IISR beams, and (2) the SO range may not exceed 1300 km. The transparent histograms with black borders show the distributions of the observed SO. One can see that the distributions of the observed and calculated SO are in good agreement up to the altitude of 700 km; however, there are altitudes where IISR observes more SO than there is in the catalogue. From the altitude of 700 km the distributions are in disagreement. This is caused by that the radar energy potential is not enough for the detection of small SO at altitudes higher than 700 km. Fig. 10 and 11 also show the altitude distribution of signal-to-noise ratio for the observed SO.

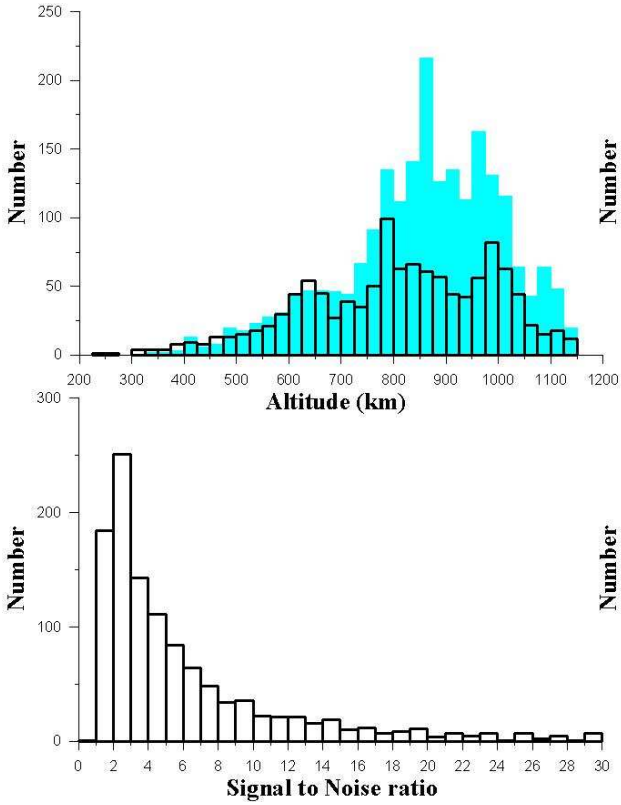

Figure 10. Top panel is altitude distribution of object numbers for 14 February 2009. The prediction is blue histogram. The observations are transparent histograms with black borders. Bottom panel is distribution of signal-to-noise ratio for the observed SO.

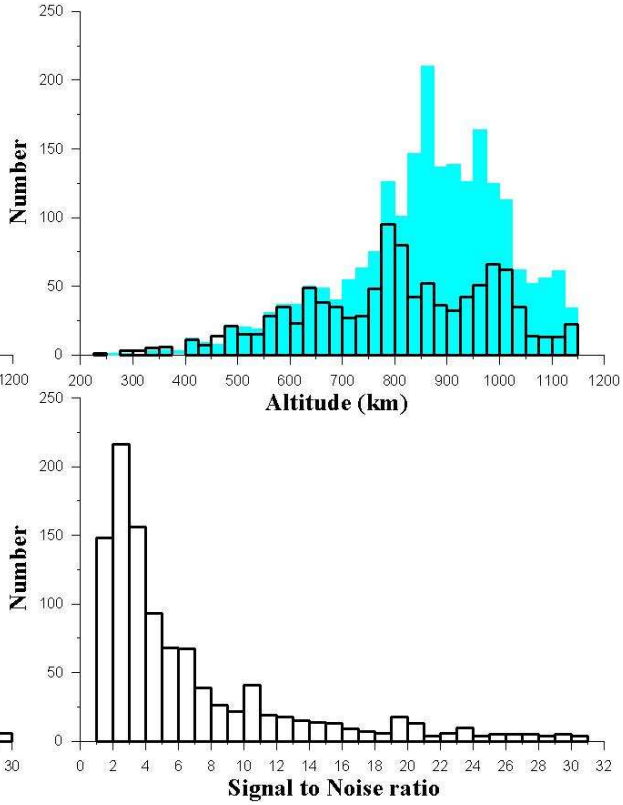

Figure 11. Top panel is altitude distribution of object numbers for 16 February 2009. The prediction is blue histogram. The observations are transparent histograms with black borders. Bottom panel is distribution of signal-to-noise ratio for the observed SO.

8. CONCLUSION

In summary, we have found that IISR standard ionospheric measurements provide obtaining the valuable space debris data. The mere amount of data, that will be available in case simultaneous operations with ionospheric measurements in the order of 3000 – 4000 h per year can be performed, provides an important contribution to the understanding of the evolution of LEO space debris.

In each sample series we measure the following coordinate characteristics: distance (R), beam velocity (V), azimuth angle (ε), SO elevation (Θ), and signal amplitude. When signal-to-noise ratio is high enough

(S/N > 10), the typical root mean square deviations for R, V, ε, and Θ are 100 m, 10 m/s, 5 angular minutes, and 5 angular minutes, respectively. This accuracy is enough for determination of the SO orbit in the next SO circuit passing through IISR sector. Two from six Keplerian elements of the orbit can be defined with high accuracy, they are the inclination and the right ascension of the ascending node of the observed SO.

Because of geographical position and technical feasibility IISR is an important facility for SD-tracking over East Siberia and Mongolia and performing SO coordinate and non-coordinate measurements.

REFERENCES

1. Landgraf M., Jehn R., Flury W. (2004). Comparison of EISCAT radar data on space debris with model predictions by the master model of ESA. *Advances in Space Research* 34, 872–877.
2. Zherebtsov, G.A., Zavorin, A.V., Medvedev, A.V., *et al.* (2002). The Irkutsk incoherent scattering radar, *Journal of Communications Technology and Electronics*, **47** (11), 1222-1228.
3. Lebedev, V.P., Medvedev, A.V., and Kushnarev, D.S. (2006) Calibration Method for Directivity Diagram of the Irkutsk IS Radar. In *Proc. IXth. BShFF Session of Young Scientists "Physical Processes in Space and near- Earth Medium"*, (Irkutsk), 185–188.
4. Levin B.R. (1974). Teoreticheskie osnovy statisticheskoy radiotehniki. Moskva: "Sovetskoe radio", 552 c.